

Oxysophoridine protects against cerebral ischemia/reperfusion injury via inhibition of TLR4/p38MAPK-mediated ferroptosis

JING ZHAO, MINGMING MA, LEI LI and GAOLI FANG

Department of Neurology, Hangzhou Red Cross Hospital, Hangzhou, Zhejiang 310003, P.R. China

Received July 19, 2022; Accepted September 8, 2022

DOI: 10.3892/mmr.2023.12931

Abstract. Oxysophoridine (OSR) is an alkaloid extracted from *Sophora alopecuroides* L. and exerts beneficial effects in cerebral ischemia/reperfusion (I/R) injury. However, the molecular mechanism underlying the regulatory effects of OSR in cerebral I/R injury remains unclear. In the present study, a cerebral I/R injury rat model was established by occlusion of the right middle cerebral artery. Hematoxylin and eosin and triphenyltetrazolium chloride staining were performed to assess histopathological changes and the extent of cerebral injury to the brain. A Cell Counting Kit-8 and TUNEL assay and western blotting were performed to assess cell viability and apoptosis. Ferroptosis and oxidative stress were evaluated based on ATP and Fe²⁺ levels and DCFH-DA staining. The protein expression levels of inflammatory factors were assessed using ELISA. The protein expression levels of members of the toll-like receptor (TLR)4/p38MAPK signaling pathway were evaluated using immunofluorescence staining and western blotting. The results demonstrated that OSR decreased brain injury and neuronal apoptosis in the hippocampus in I/R-induced rats. OSR inhibited reactive oxygen species (ROS) production, decreased levels of ATP, Fe²⁺ and acyl-CoA synthetase long-chain family member 4 (ACSL4) and transferrin 1 protein and increased the protein expression levels of ferritin 1 and glutathione peroxidase 4. Furthermore, OSR blocked TLR4/p38MAPK signaling in brain tissue in the I/R-induced rat. *In vitro* experiments demonstrated that TLR4 overexpression induced generation of ROS, ATP and Fe²⁺, which promoted the expression of ferroptosis-associated proteins in hippocampal HT22 neuronal cells. The ferroptosis inducer erastin decreased the effects of OSR on oxygen-glucose deprivation/reoxygenation (OGD/R)-induced cell viability, oxidative stress and inflammatory response. Together, the

results demonstrated that OSR alleviated cerebral I/R injury via inhibition of TLR4/p38MAPK-mediated ferroptosis.

Introduction

Ischemic cerebrovascular disease, which accounts for 70% of all strokes worldwide, is associated with high morbidity and mortality rates (1-3). At present, the primary clinical treatment for ischemic cerebrovascular disease is reperfusion of the affected area as soon as possible (4). However, when the blood supply is restored, the resultant damage to the brain tissue and the nervous system, termed cerebral ischemia/reperfusion (I/R) injury, is a key issue in the clinical treatment of ischemic cerebrovascular disease (5). Moreover, it is difficult to treat cerebral I/R injury due to the complicated pathological processes and the multiple mechanisms involved (6). At present, clinical interventional treatment and drugs primarily used in cerebral I/R injury therapy include thrombolytics, calcium channel antagonists, free-radical scavengers and excitatory amino acid regulators (7). However, the narrow therapeutic temporal window and single target approach result in a limited efficacy of treatment for cerebral I/R injury (8). Therefore, there is an urgent need to find novel therapies to improve the therapeutic outcomes following cerebral I/R injury.

Oxysophoridine (OSR) is one of the primary alkaloids extracted from *Sophora alopecuroides* L. (9). Previous studies have reported that OSR has certain pharmacological properties in regard to sedation, anti-inflammatory effects, arrhythmia and immune regulation (10,11). Furthermore, OSR has favorable preventative and therapeutic effects on heart failure, myocardial infarction, cerebral ischemia and I/R injury and other cardiovascular and cerebrovascular disease (11). Cao *et al* (12) reported that OSR protects against exacerbated spinal cord injury via its anti-inflammatory, anti-oxidative and anti-apoptotic effects. Another previous study reported that OSR has a neuroprotective effect on mice with cerebral I/R injury by suppressing oxidative stress and expression of the N-methyl-D-aspartate receptor subunit NR1 (13). However, the functional roles and molecular mechanism of OSR on cerebral I/R injury are incompletely understood. Therefore, in the present study, the effect of OSR in cerebral I/R injury was evaluated.

Materials and methods

Animal care and experimental groups. The present study was approved by the Animal Care and Use Committee of

Correspondence to: Dr Jing Zhao, Department of Neurology, Hangzhou Red Cross Hospital, 208 Eastern Ring Road, Hangzhou, Zhejiang 310003, P.R. China
E-mail: zhaojingzj13@163.com

Key words: oxysophoridine, cerebral ischemia-reperfusion, TLR4, p38MAPK, ferroptosis

Hangzhou Red Cross Hospital (Hangzhou, China; approval no. 20220414) and performed in accordance with Chinese legislation regarding the use of experimental animals. A total of 30 adult male Sprague-Dawley rats (7 weeks old) weighing 280–320 g were purchased from the Laboratory Animal Resources, Chinese Academy of Sciences. The rats were housed at a room temperature of $21\pm 2^{\circ}\text{C}$ and $55\pm 5\%$ relative humidity with a 12/12-h light/dark cycle and free access to standard chow and tap water. After one week, the cerebral I/R injury model was established using improved thread occlusion of the right middle cerebral artery (MCAO) model as described previously (14). Briefly, rats were anesthetized by intraperitoneal administration of 2.25% pentobarbital sodium (45 mg/kg) for 2 h, a midline cervical incision was made, the MCA was located and its branches were ligated. The induction of ischemia was performed by occluding the right internal carotid artery using a thread. Following transient MCAO for 2 h, the nylon thread was removed to allow the return of blood flow through the right internal carotid artery. Rats in the control group underwent the same surgical procedure but the right internal carotid artery was not occluded. Rats were randomly divided into five groups ($n=6$) as follows: Healthy control group that was subjected to a sham operation (control); cerebral I/R injury group that underwent MCAO for 2 h followed by reperfusion for 24 h (I/R) and I/R + OSR groups which were administered 60, 120 or 180 mg/kg OSR intraperitoneally once/day for 7 days before MCAO. The total duration of the experiment was 10 days. All rats were euthanized using intraperitoneal administration of pentobarbital sodium (200 mg/kg) 24 h after reperfusion. The humane endpoints of this experiment were as follows: Marked decrease in food or water intake, labored breathing, inability to stand or no response to external stimuli. No humane endpoints of the experiment were reached by any of the rats during the experiment. Death was verified by lack of heartbeat and a cold body. No animals were found dead before the end of the experiment.

Histopathological examination. The brain tissue from rats in five groups was fixed with 10% neutral formaldehyde buffer at 4°C overnight, dehydrated in a series of graded concentrations of ethanol, embedded in paraffin and cut into $4\ \mu\text{m}$ sections. The sections were stained using hematoxylin for 6 min and 1% eosin for 2 min, both at room temperature. A light microscope was used to assess the pathological changes in the samples following I/R treatment at a magnification of $\times 400$.

2,3,5-triphenyltetrazolium chloride (TTC) staining. Rat brains were dissected into 2 mm coronal slices and incubated in 2% TTC (Beijing Solarbio Science & Technology Co., Ltd.) at 37°C for 10 min. Following TTC staining, the normal brain tissue stained dark red and the infarcted tissue was unstained (white). The tissue was fixed in 4% paraformaldehyde (Beyotime Institute of Biotechnology) for 24 h at 4°C and imaged using a digital camera (Canon, Inc.). The infarcted volume was calculated as follows: Infarcted volume (%) = (volume of white sections/volume of the whole brain) $\times 100$.

Measurement of ATP and Fe^{2+} levels. ATP levels in brain tissues and HT22 cells were assessed using the CellTiter-Glo Luminescent Assay kit (Promega Corporation) according

to the manufacturer's protocol. Fe^{2+} levels in brain tissue and HT22 cells were evaluated using an Iron Assay kit (cat. no. ab83366; Abcam) according to the manufacturer's protocol. The absorbance at 520 nm was assessed for the determination of iron concentration.

Immunofluorescence staining. Brain sections ($10\ \mu\text{m}$) that were stored at -18°C were permeabilized using 0.5% Triton X-100 at room temperature for 30 min and blocked using 10% bovine serum albumin (Thermo Fisher Scientific, Inc.) for 1 h at room temperature. Subsequently, brain tissue was incubated with primary antibodies against toll-like receptor (TLR)4 (1:1,000; cat. no. ab22048; Abcam) at 4°C overnight. The cells were exposed to DAPI (BIOSS) at room temperature for 5 min were then cultivated with a secondary Alexa Fluor[®] 488-conjugated goat anti-mouse antibody (1:1,000; cat. no. ab150113; Abcam) at room temperature in the dark for 1 h. Finally, the sections were rinsed with phosphate-buffered saline (Beyotime Institute of Biotechnology) and imaged using a fluorescence microscope (magnification, $\times 400$; Leica Microsystems GmbH).

Cell culture and treatment. The hippocampal HT22 neuronal cell line was purchased from the Ningbo Mingzhou Biotechnology Co., Ltd. The cells were cultured in DMEM (Gibco; Thermo Fisher Scientific, Inc.) supplemented with 10% FBS (HyClone, Cytiva), 100 U/ml penicillin and 100 $\mu\text{g}/\text{ml}$ streptomycin (both Gibco; Thermo Fisher Scientific, Inc.) in a humidified incubator with 5% CO_2 at 37°C . To establish an *in vitro* oxygen-glucose deprivation/reoxygenation (OGD/R) model, HT22 cells were cultured in glucose-free DMEM (Wuhan Procell Life Science & Technology Co., Ltd.) in an oxygen-free incubator supplied with 5% CO_2 and 95% N_2 at 37°C for 2 h. Following hypoxia treatment, the media was replaced with normoxic glucose-containing medium and cells were transferred to an incubator supplied with 95% air and 5% CO_2 at 37°C for 24 h. Cells were incubated with OSR (10, 20 or 40 nM) for 48 h at room temperature before OGD/R challenge. Subsequently, the indicated cells were treated with 5 μM anisomycin (a novel and specific p38MAPK activator; MedChemExpress) at room temperature for 1 h or 1 μM erastin (a ferroptosis inducer; Shanghai Aladdin Biochemical Technology Co., Ltd.) at room temperature for 24 h.

Cell transfection. TLR4-specific pcDNA overexpression vector (Oe-TLR4) or pcDNA3.1 empty vector, which served as the negative control (Oe-NC), was purchased from Shanghai Genechem Co., Ltd. A total of 100 nM plasmids were transfected into HT22 cells using Lipofectamine[®] 2000 reagent (Invitrogen; Thermo Fisher Scientific, Inc.) for 48 h at 37°C . Following 48 h of transfection, cells were collected for use in subsequent experiments.

Reverse transcription-quantitative PCR (RT-qPCR). Total RNA was extracted from HT22 cells using TRIzol[®] reagent (Invitrogen; Thermo Fisher Scientific, Inc.) according to the manufacturer's protocol. The quality and concentration of RNA were assessed using NanoDrop 2000 (Shanghai Aiyuan Biotechnology Co., Ltd.) based on the ratio of absorbance at 260 and 280 nm. A PrimeScript[™] RT Reagent kit (Takara

Bio, Inc.) was used to reverse-transcribe 2 μg RNA into cDNA using the thermocycling protocol as follows: 25°C for 5 min, 42°C for 30 min, 85°C for 5 min and then held at 4°C for 5 min. Amplification of the cDNA was performed using qPCR using an SYBR Premix Ex Taq™ II kit (Takara Bio, Inc.). The thermocycling protocol was 95°C for 3 min, followed by 35 cycles of denaturation at 95°C for 30 sec, annealing at 60°C for 30 sec and extension at 72°C for 1 min. A final extension step at 72°C for 7 min was performed in each PCR assay. The primer sequences used for PCR were as follows: TLR4 forward (F), 5'-CCCATGCATTTGGCCTTAGC-3' and reverse (R), 5'-AGA GCACTGAACCTCCTTGC-3'; and GAPDH (F), 5'-GTCGTG GAGTCTACTGGCGTCTTCA-3' and (R), 5'-TCGTGGTTC ACACCCATCACAAACA-3'. The relative mRNA levels were normalized to GAPDH using the $2^{-\Delta\Delta C_q}$ method (15).

Cell Counting Kit-8 (CCK-8) assay. Following various treatments, cells were plated at a density of 5×10^3 cells/well in 96-well plates and cultured in DMEM with 10% FBS (Gibco; Thermo Fisher Scientific, Inc.) at 37°C for 24 h. A total of 10 μl CCK-8 solution (Beyotime Institute of Biotechnology) was added to each well and incubated for 2 h. The absorbance at 450 nm was assessed using a microplate reader (Bio-Rad Laboratories, Inc.). All experiments were performed in triplicate with five independent repeats.

ELISA. IL-1 β , TNF- α and IL-10 protein expression levels in HT22 cells were assessed using ELISA kits (cat. nos. EK0393, EK0526 and EK0418 respectively; Wuhan Boster Biological Technology, Ltd.) according to the manufacturer's protocols. The absorbance was assessed at 450 nm using a microplate reader (BioTek Instruments, Inc.).

Measurement of oxidative stress. To assess reactive oxygen species (ROS) generation, DCFH-DA staining (cat. no. D6883; MilliporeSigma) was used. HT22 cells were washed with PBS and incubated with 10 μM DCFH-DA in the dark for 30 min at 37°C. After washing three times with PBS, fluorescence images were obtained using an Axio-Observer-D1 fluorescence microscope (ZEISS AG; magnification, x400). Furthermore, the activity of superoxide dismutase (SOD) and levels of malondialdehyde (MDA) and catalase (CAT) were assessed using SOD assay kit (cat. no. S0101M), MDA assay kit (cat. no. S0131S) and CAT assay kit (cat. no. S0051), all of which were obtained from Beyotime Institute of Biotechnology. The absorbance at 532 nm was assessed using a Benchmark microplate reader (Bio-Rad Laboratories, Inc.).

TUNEL assay. TUNEL assay was performed to evaluate the degree of apoptosis in tissue and cells. Following fixation with 4% paraformaldehyde at room temperature for 30 min, tissue sections or cells were incubated with proteinase K at room temperature for 15 min, placed in 3% H₂O₂ for 15 min at room temperature and treated using a TUNEL detection kit for 60 min at 37°C. Following incubation, the PBS-rinsed cells were co-labeled with 1 $\mu\text{g}/\text{ml}$ DAPI working solution for 10 min at 37°C. The positive cells were mounted with fluorescent mounting media (Beijing Solarbio Science & Technology Co., Ltd.) and analyzed using ImageJ 1.8.0 software (National Institutes of Health). More than 10 fields of view/section for

each sample were assessed. The labeled cells were visualized using an Olympus BX53 fluorescence microscope (magnification, x100; Olympus Corporation).

Western blotting. Total protein was extracted from tissue and cells using RIPA lysis buffer (Beyotime Institute of Biotechnology) and then quantified with bicinchoninic acid (BCA) protein assay kit (cat. no. P0012S; Beyotime Institute of Biotechnology). An equal amount of protein (60 $\mu\text{g}/\text{lane}$) was separated on 10% SDS gels and then transferred to a nitrocellulose blotting membrane (Pall Life Sciences). The membranes were blocked with 5% non-fat milk dissolved in 0.1% TBS-T buffer for 2 h at room temperature and probed with primary antibodies as follows: Bax (1:1,000; ab32503), Bcl-2 (1:1,000; ab196495), acyl-CoA synthetase long-chain family member 4 (ACSL4; 1:1,000; ab155282), transferrin 1 (TFR1; 1:1,000; ab269513), ferritin 1 (FTH1; 1:1,000; ab1837810), glutathione peroxidase 4 (GPX4; 1:1,000; ab252833), TLR4 (1:1,000; ab217274), MyD88 (1:1,000; ab219413), phosphorylated (p)-p38 (1:1,000; ab4822), p38 (1:1,000; ab170099), inducible nitric oxide synthase (iNOS; 1:1,000; ab178945), cyclooxygenase 2 (COX-2; 1:1,000; ab179800), p-p65 (1:1,000; ab76302), p65 (1:1,000; ab32536) and GAPDH (1:1,000; ab8245; all Abcam) overnight at 4°C. The membranes were incubated with HRP-conjugated anti-mouse or anti-rabbit secondary antibodies (1:2,000, ab6789 and ab6721, respectively; Abcam) for 2 h at room temperature. Signals were visualized using enhanced chemiluminescence reagent (Thermo Fisher Scientific, Inc.) according to the manufacturer's instructions. Densitometry analysis was performed using ImageJ (Version 1.49; National Institutes of Health).

Statistical analysis. Statistical analysis was performed using SPSS version 17.0 (SPSS, Inc.) and data are presented as the mean \pm SD. Comparisons between multiple groups were performed using one-way ANOVA followed by Bonferroni's post hoc test for multiple comparisons. All cellular experiments were performed ≥ 3 times from three different cultures. $P < 0.05$ was considered to indicate a statistically significant difference.

Results

OSR alleviates brain injury and neuronal apoptosis in I/R-induced rats. The structure was presented in Fig. 1A. To evaluate the role and mechanism of OSR in cerebral I/R injury, an *in vivo* cerebral I/R injury model was established using MCAO. Control group demonstrated a clear outline of cortex neurons, a compact structure and abundant cytoplasm (Fig. 1B). However, I/R injury resulted in pyknotic and shrunken nuclei, nuclear loss and numerous vacuolated spaces. These pathological changes were restored following OSR preconditioning in a dose-dependent manner. Furthermore, I/R treatment significantly increased the infarct volume compared with the control while OSR led to a decrease in cerebral infarct volume compared with the I/R group (Fig. 1C and D). TUNEL assay demonstrated that the apoptotic rate of hippocampal neurons in I/R-induced rats was increased compared with the control; however, the apoptotic rate was markedly decreased after administration of OSR compared with the I/R group (Fig. 1E).

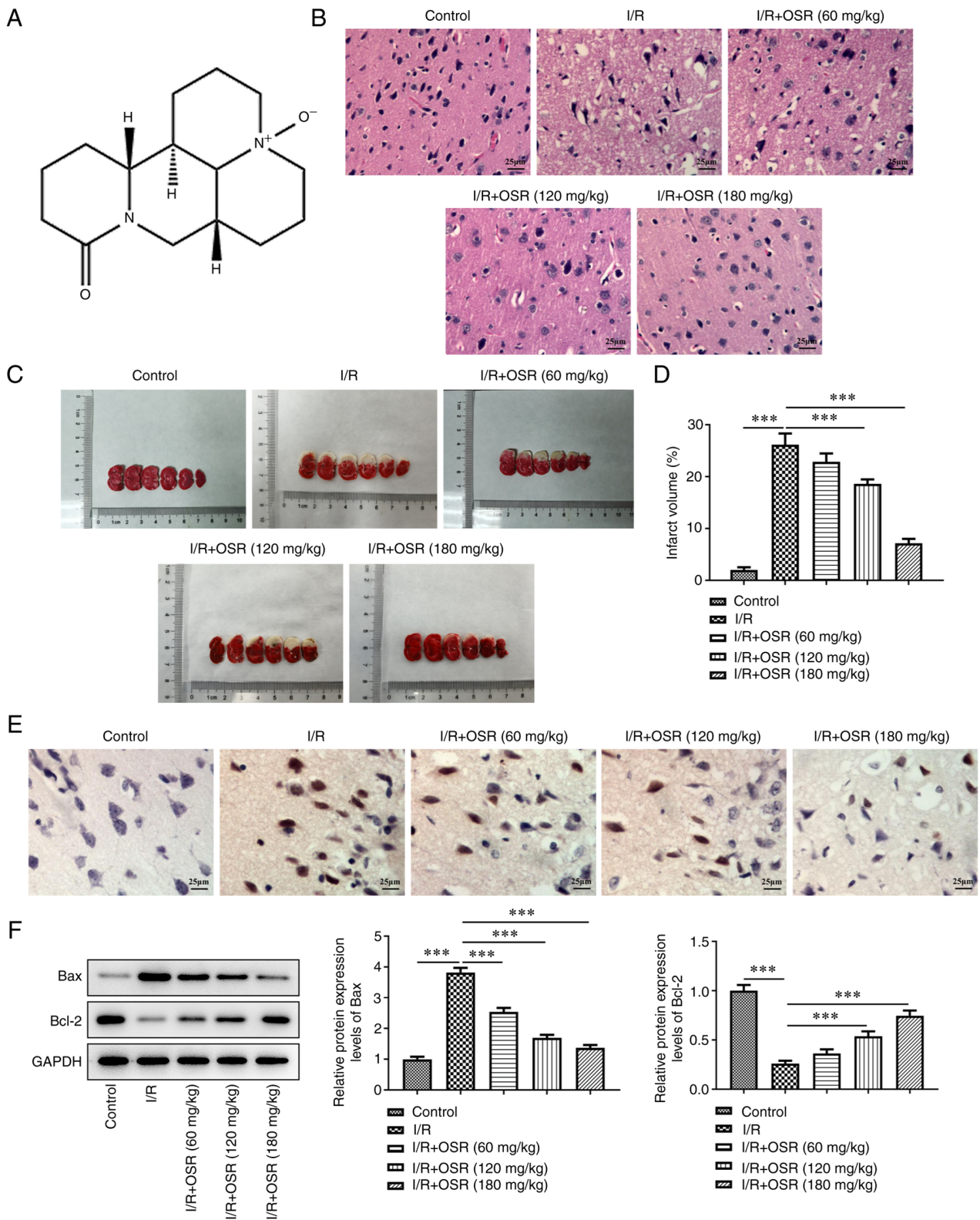


Figure 1. OSR alleviates brain injury and neuronal apoptosis in I/R-induced rats. (A) Structure of OSR. (B) Pathological changes in rat brain tissue was assessed using hematoxylin and eosin staining. Scale bar, 25 μ m. (C) Representative brain sections with the largest volume infarction were assessed using 2,3,5-triphenyltetrazolium chloride staining. (D) Infarct volume. (E) Apoptosis rate was assessed using TUNEL assay. Scale bar, 25 μ m. (F) Protein expression levels of Bax and Bcl-2 were semi-quantified using western blotting. Data are presented as mean \pm SD. Comparisons between multiple groups were performed using one-way ANOVA followed by Bonferroni's post hoc test for multiple comparisons. *** P <0.001. OSR, oxySphoridine; I/R, ischemia/reperfusion.

Western blotting results demonstrated that I/R resulted in a significant increase in Bax protein expression levels and a significant decrease in the protein expression levels of Bcl-2

compared with the control (Fig. 1F). Nevertheless, OSR treatment cut down Bax protein and elevated Bcl-2 content concentration-dependently relative with the I/R group.

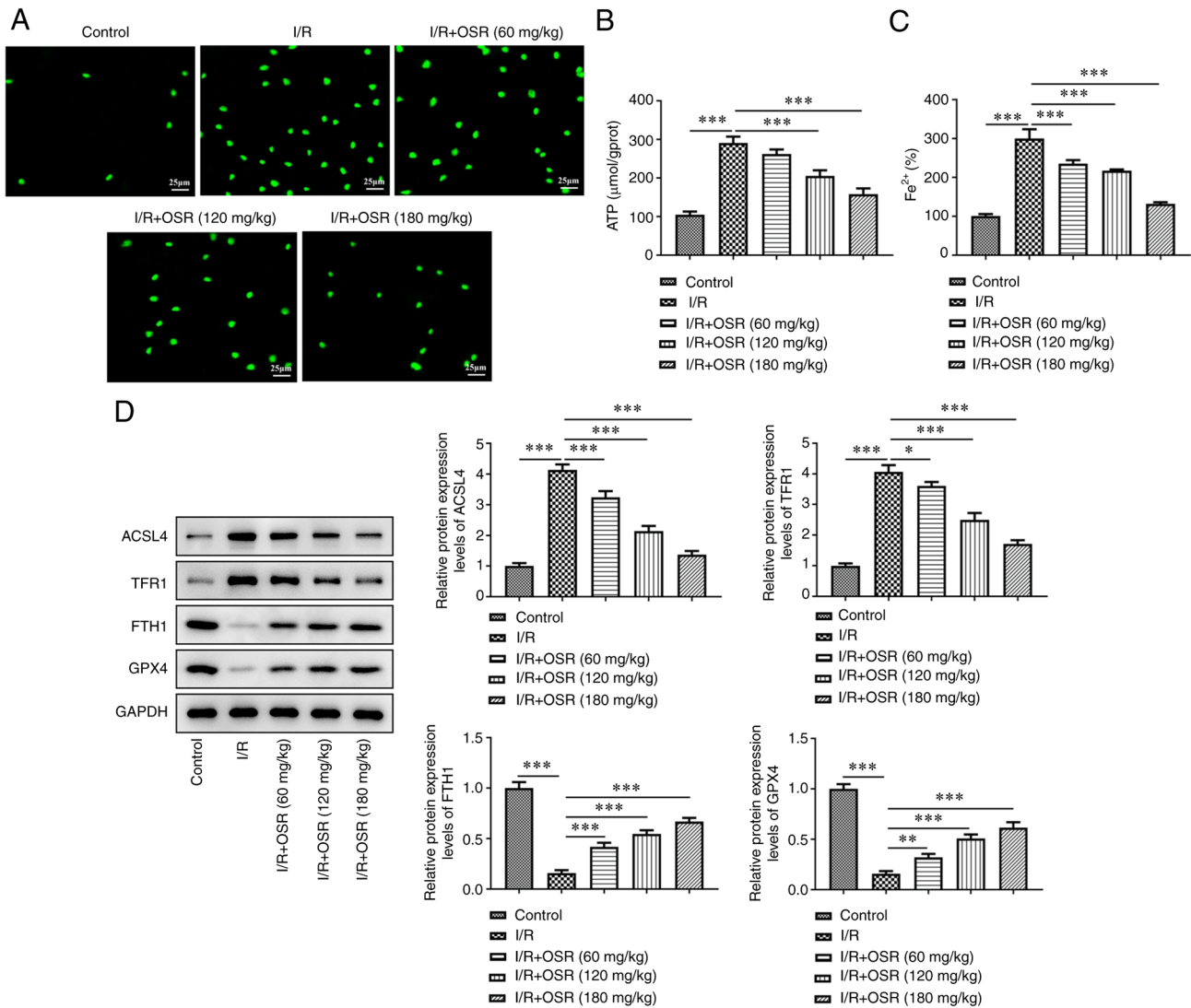


Figure 2. OSR decreases ROS accumulation and ferroptosis induced by I/R in rat brain. The levels of (A) ROS, (B) ATP and (C) Fe²⁺ were assessed in I/R rat brain tissue. The control was set as 100%. Scale bar, 25 μm. (D) Protein expression levels of ACSL4, TFR1, FTH1 and GPX4 were semi-quantified using western blotting. Data are presented as mean ± SD. Comparisons between multiple groups were performed using one-way ANOVA followed by Bonferroni's post hoc test for multiple comparisons. *P<0.05, **P<0.01 and ***P<0.001. ROS, reactive oxygen species; OSR, oxysphoridine; I/R, ischemia/reperfusion; TFR1, transferrin 1; FTH1, ferritin 1; GPX4, glutathione peroxidase 4; ACSL4, acyl-CoA synthetase long-chain family member.

OSR decreases ROS accumulation and ferroptosis induced by I/R in rat brain tissue. I/R induction elevated ROS levels in brain tissue of rats; however, OSR treatment markedly decreased accumulation of ROS (Fig. 2A). Moreover, compared with the control group, the I/R group demonstrated significantly higher levels of ATP, whereas decreased levels of ATP were observed in the OSR intervention group compared with the I/R group (Fig. 2B). Consistently, I/R significantly increased levels of Fe²⁺ compared with the control and OSR pretreatment significantly decreased the increased levels of Fe²⁺ (Fig. 2C). Furthermore, a significant increase in protein expression levels of ACSL4 and TFR1 and a significant decrease in protein expression levels of FTH1 and GPX4 were observed in the I/R group compared with the control group. OSR treatment significantly dose-dependently reversed the effects of I/R on expression levels of these proteins in the brain tissue of rats with I/R injury (Fig. 2D).

OSR inhibits TLR4/p38MAPK signaling in brain tissue of I/R-induced rats. To evaluate the mechanism of action of OSR in I/R-induced rats, the activity of the TLR4/p38MAPK signaling pathway was assessed. Immunofluorescence staining demonstrated that the number of positive cells was markedly higher in the I/R group compared with the control group and that OSR markedly decreased the number of positive cells compared with the I/R group, which indicated that levels of TLR4 decreased following OSR treatment (Fig. 3A). Furthermore, western blotting demonstrated that I/R significantly enhanced protein expression levels of TLR4, MyD88 and p-p38 compared with the control and the changes were significantly reversed by OSR treatment (Fig. 3B).

OSR suppresses OGD/R-induced neuronal ferroptosis by inhibiting TLR4/p38MAPK signaling. To evaluate the role of TLR4/p38MAPK signaling in the regulation of OSR in cerebral I/R injury, an *in vitro* cerebral I/R injury model was

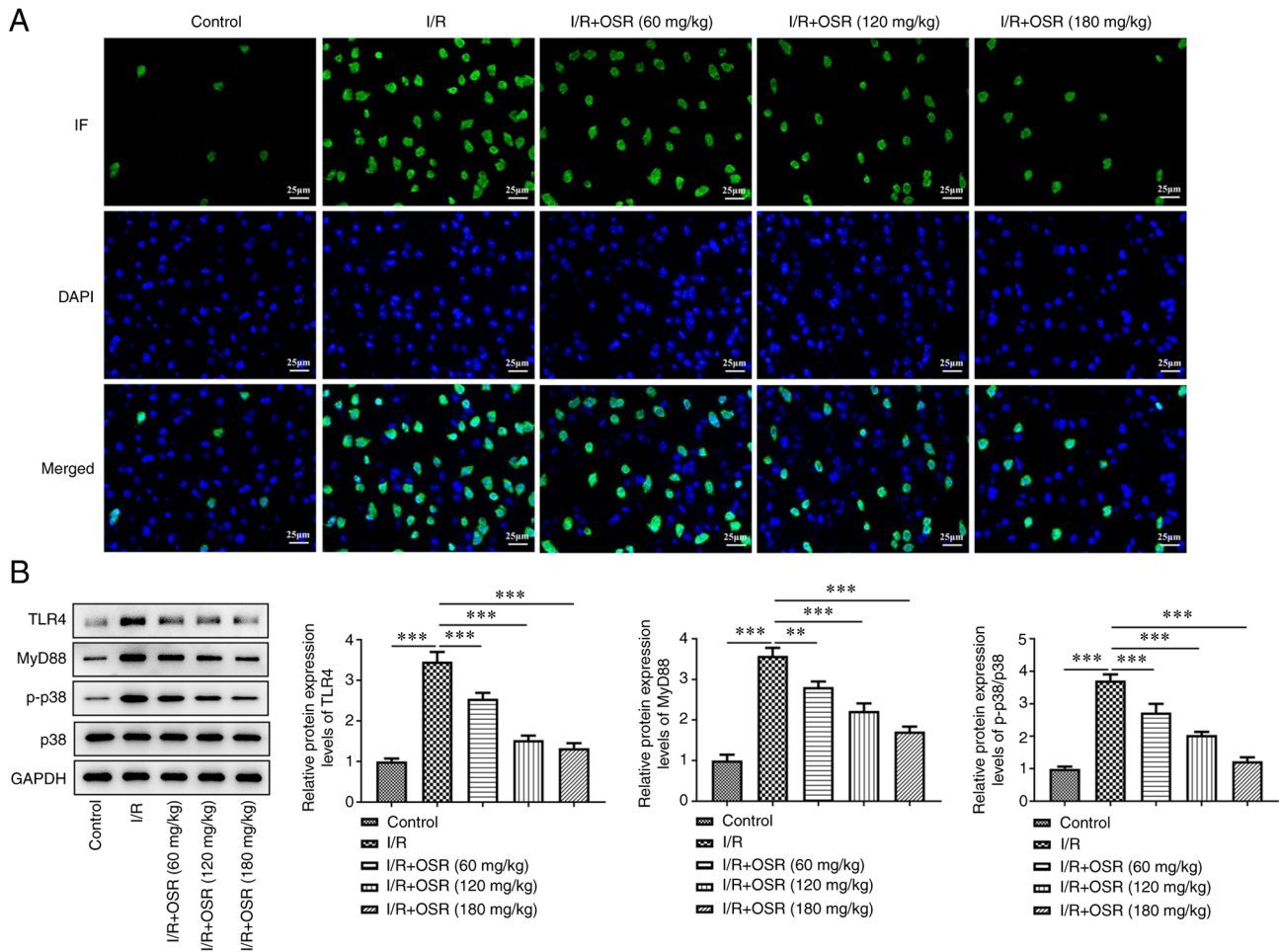


Figure 3. OSR inhibits TLR4/p38MAPK signaling in brain tissue of I/R-induced rats. (A) Protein expression levels of TLR4 in brain tissue of I/R-induced rats were evaluated using immunofluorescence staining. Scale bar, 25 μ m. (B) Protein expression levels of TLR4, MyD88, p-p38 and p38 were semi-quantified using western blotting. Data are presented as mean \pm SD. Comparisons between multiple groups were performed using one-way ANOVA followed by Bonferroni's post hoc test for multiple comparisons. ** P <0.01 and *** P <0.001. OSR, oxsyphoridine; I/R, ischemia/reperfusion; p, phosphorylated; TLR, toll-like receptor; IF, immunofluorescence staining.

established using OGD/R. The protein expression levels of TLR4, MyD88 and p-p38 in HT22 cells were significantly increased following I/R exposure compared with the control group and OSR significantly decreased expression levels of these proteins compared with the OGD/R group (Fig. 4A). TLR4 was overexpressed in HT22 cells and transfection efficiency was assessed using RT-qPCR and western blotting. As depicted in Fig. 4B and C, the mRNA and protein expressions of TLR4 were significantly increased in Oe-TLR4 group when compared with those in Oe-NC group. Cells were treated with OSR (40 μ M) and 5 μ M p38MAPK agonist anisomycin was added to cells. OGD/R treatment markedly elevated the levels of ROS compared with the control and OSR markedly counteracted these effects (Fig. 4D). However, TLR4 overexpression and anisomycin both abated the effects of OSR treatment. Furthermore, levels of ATP and Fe²⁺ were significantly increased by OGD/R while OSR significantly suppressed the OGD/R-induced increase in ATP and Fe²⁺ levels in the OGD/R + OSR group compared with the OGD/R group. TLR4 overexpression and anisomycin significantly reversed the effects of OSR on the levels of ATP and Fe²⁺ compared with the OGD/R + OSR + Oe-NC and OGD/R + OSR groups, respectively (Fig. 4E and F). OGD/R was

demonstrated to significantly increase protein expression levels of ACSL4 and TFR1 and significantly decrease protein expression levels of FTH1 and GPX4 compared with the control and OSR significantly reversed these trends compared with the OGD/R group. Moreover, TLR4 overexpression and anisomycin treatment both significantly reversed the effects of OSR on these ferroptosis-associated proteins compared with the OGD/R + OSR + Oe-NC and OGD/R + OSR groups, respectively (Fig. 4G and H).

Erastin decreases the protective effect of OSR on viability in OGD/R-induced cells. To study the role of ferroptosis in OGD/R induced cells, the ferroptosis inducer erastin was used. OGD/R significantly decreased cell viability compared with the control, whereas OSR significantly reversed this effect compared with OGD/R group and cell viability was markedly decreased by erastin (Fig. 5A). TUNEL assay demonstrated a marked increase in the rate of cell apoptosis following OGD/R treatment compared with the control and OSR markedly inhibited apoptosis in OGD/R-induced cells compared with the OGD/R group; however, erastin markedly accelerated cell apoptosis rate (Fig. 5B and C). Furthermore, OGD/R significantly increased Bax protein expression levels and decreased

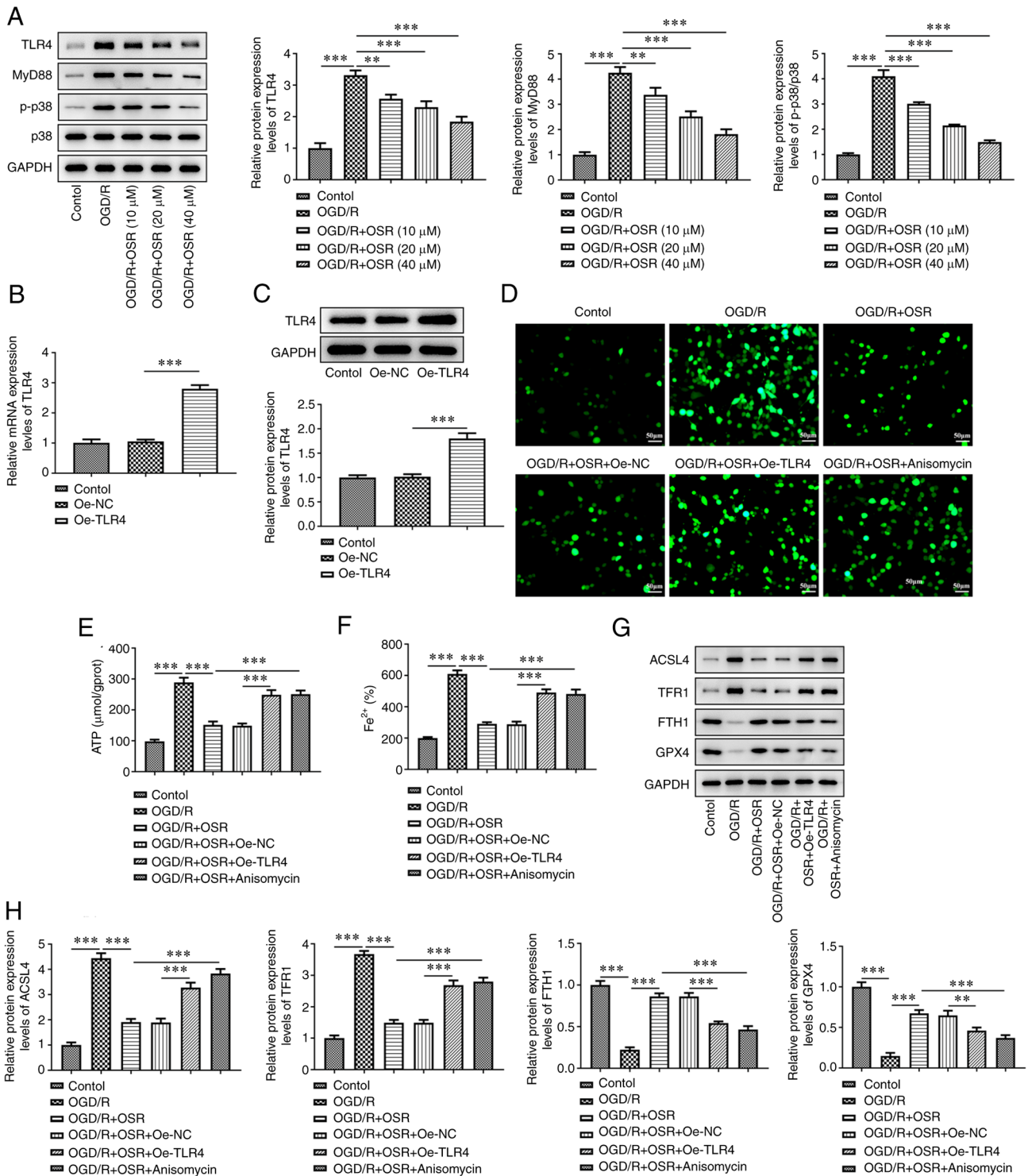


Figure 4. OSR suppresses OGD/R-induced neuronal ferroptosis by inhibiting TLR4/p38MAPK signaling. (A) Protein expression levels of TLR4, MyD88, p-p38 and p38 were semi-quantified using western blotting. (B) mRNA and (C) protein expression levels of TLR4 in OGD/R-induced cells were assessed using reverse transcription-quantitative PCR and western blotting, respectively. The levels of (D) reactive oxygen species, (E) ATP and (F) Fe²⁺ were assessed in OGD/R-induced cells. Scale bar, 50 μ m. (G) Protein expression levels of ACSL4, TFR1, FTH1 and GPX4 were (H) semi-quantified using western blotting. Data are presented as mean \pm SD. Comparisons between multiple groups were performed using one-way ANOVA followed by Bonferroni's post hoc test for multiple comparisons. ***P<0.01 and ****P<0.001. OGD/R, oxygen-glucose deprivation/reoxygenation; I/R, ischemia/reperfusion; p, phosphorylated; Oe, overexpression; NC, negative control; OSR, oxsophoridine; TLR, toll-like receptor; TFR1, transferrin 1; FTH1, ferritin 1; GPX4, glutathione peroxidase 4; ACSL4, acyl-CoA synthetase long-chain family member.

Bcl-2 protein expression levels compared with the control, whereas OSR significantly reversed the expression levels of these two proteins compared with the OGD/R group. Erastin demonstrated the inverse effect on these protein expression

levels, evidenced by increased Bax protein expression level and decreased Bcl-2 protein expression level in OGD/R + OSR + Erastin group compared with the OGD/R + OSR group (Fig. 5D).

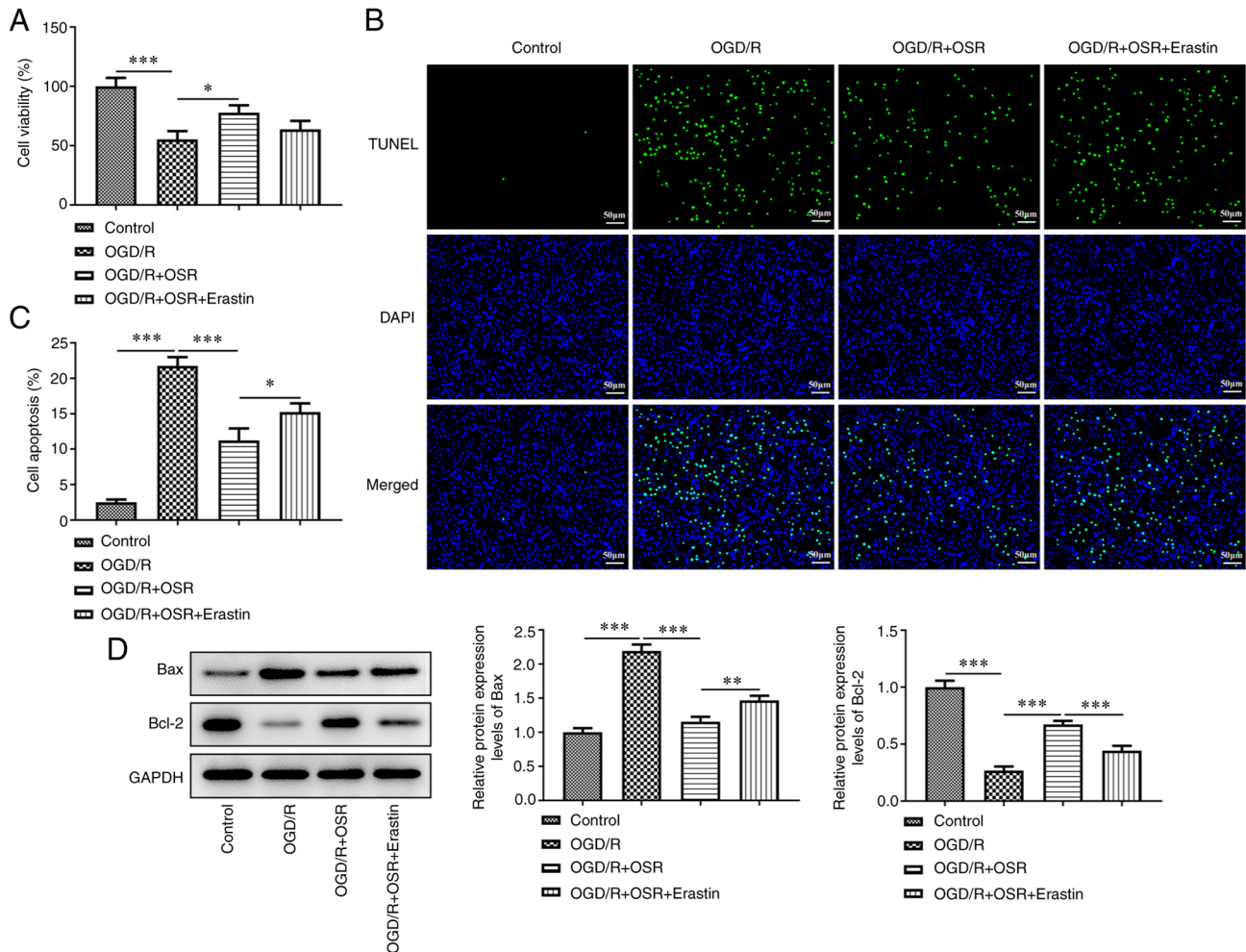


Figure 5. Erastin decreases the protective effect of OSR on cellular viability in OGD/R-induced cells. (A) Viability of OGD/R-induced cells treated with or without OSR and/or Erastin were assessed using Cell Counting Kit-8 assay. (B) Apoptosis rate was assessed using TUNEL assay and then (C) quantified. Scale bar, 50 μ m. (D) Protein expression levels of Bax and Bcl-2 were semi-quantified using western blotting. Data are presented as mean \pm SD. Comparisons between multiple groups were performed using one-way ANOVA followed by Bonferroni's post hoc test for multiple comparisons. * P <0.05, ** P <0.01 and *** P <0.001. OGD/R, oxygen-glucose deprivation/reoxygenation; OSR, oxysphoridine.

Erastin decreases the inhibitory effect of OSR on OGD/R-induced oxidative stress and inflammatory response. OGD/R led to a significant decrease in SOD activity and CAT levels, but significantly increased MDA levels compared with the control. OSR treatment significantly enhanced the levels of SOD and CAT and significantly reduced the levels of MDA compared with the OGD/R group; however, this was significantly reversed by the addition of erastin compared with the OGD/R + OSR group (Fig. 6A). Furthermore, protein expression levels of the proinflammatory factors IL-1 β and TNF- α were significantly elevated and the protein expression levels of anti-inflammatory factor IL-10 were significantly decreased following OGD/R exposure compared with the control. OSR pretreatment significantly reversed the effect of OGD/R on the protein expression levels of inflammatory factors compared with the OGD/R group (Fig. 6B). However, erastin significantly reversed the effects of OSR on the aforementioned inflammatory factors compared with the OGD/R + OSR group. Furthermore, OGD/R significantly increased protein expression levels of iNOS, COX-2 and p-p65 compared with the control. However, OSR significantly inhibited the expression

levels of these proteins compared with the OGD/R group and this inhibitory effect was significantly reversed following treatment with erastin compared with the OGD/R + OSR group (Fig. 6C).

Discussion

Cerebrovascular disease is one of the primary conditions associated with notable risk to human health and survival (16). Cerebral ischemia results in decreased cerebral blood flow and insufficient blood oxygen supply to brain tissue due to vascular thrombosis, resulting in brain cell damage (17,18). Therefore, it is of importance to restore blood flow to the ischemic area as soon as possible using thrombolytics or mechanical recanalization (19). However, while recanalizing occlusive cerebrovascular arteries, these treatments often aggravate the pathological damage to ischemic tissue and the nervous system and worsen the clinical symptoms, a well-established concept termed cerebral I/R injury (20). In the present study, the effect of OSR on protecting against cerebral I/R injury was assessed using a cerebral I/R injury model *in vivo* and *in vitro* and it was demonstrated that the protective role of OSR may

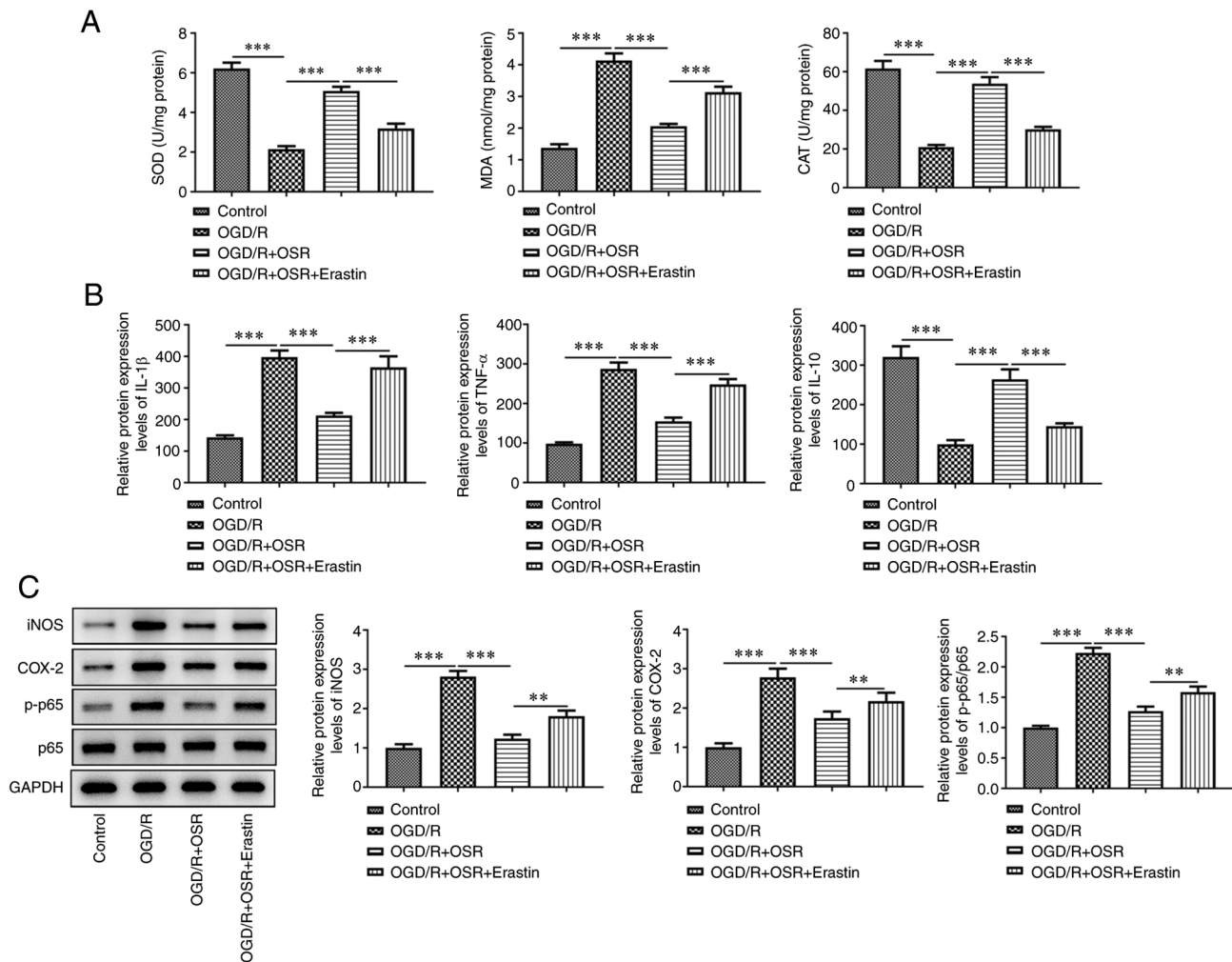


Figure 6. Erastin decreases the inhibitory effect of OSR on OGD/R-induced oxidative stress and inflammatory response. (A) Levels of SOD, MDA and CAT were assessed using specific detection kits. (B) Protein expression levels of IL-1 β , TNF- α and IL-10 were assessed using ELISA. (C) Protein expression levels of iNOS, COX-2, p-p65 and p65 were semi-quantified using western blotting. Data are presented as mean \pm SD. Comparisons between multiple groups were performed using one-way ANOVA followed by Bonferroni's post hoc test for multiple comparisons. ** P <0.01 and *** P <0.001. OSR, oxysophoridine; OGD-R, oxygen-glucose deprivation/reoxygenation; SOD, superoxide dismutase; MDA, malondialdehyde; CAT, catalase; iNOS, inducible nitric oxide synthase; COX-2, cyclooxygenase 2; p, phosphorylated.

be associated with inhibition of ferroptosis mediated by the TLR4/p38MAPK signaling pathway.

Studies have reported that Traditional Chinese Medicine can intervene in the pathological process of cerebral I/R injury by affecting multiple targets and/or pathways. For example, galangin represses the ferroptosis in hippocampal tissue of gerbils by activating the SLC7A11/GPX4 axis, thus protecting against cerebral I/R injury (21). Wang *et al* hypothesized that schizandrin protects neurons from cerebral ischemia by regulating the AMPK-mTOR pathway (22). The above findings suggested TCM possesses unique advantages and potential in the treatment of cerebral I/R injury. OSR is an alkaloid found in *Sophora alopecuroides* L, that has extensive anti-inflammatory and anti-apoptotic properties and has been reported to exhibit protective effects in spinal cord, brain and hippocampal neuron injury induced by I/R (12,23). Rui *et al* (24) reported that OSR markedly decreases neurological deficit score, neuronal damage and apoptosis and is therefore regarded as a potential neuroprotective agent for cerebral ischemia injury. Wang *et al* (25) evaluated the effects of OSR in decreasing

ischemic cerebral injury using an MCAO mouse model and reported that the neuroprotective effect of OSR was associated with inhibition of oxidative stress and apoptosis. In the present study, it was demonstrated using hematoxylin and eosin and TTC staining that OSR decreased brain injury and inhibited neuronal apoptosis based on significantly decreased Bax protein expression levels and significantly increased Bcl-2 protein expression levels in I/R-induced rats and hippocampal neuronal HT22 cells, which was consistent with previous reports (24,25).

The activation of innate immune receptors such as TLRs serves an important role in induction of inflammatory responses; TLR4 was the first mammalian TLR recognized (26). Previous studies have reported that TLR4 expression is upregulated following cerebral I/R and that this is alleviated in TLR4-deficient mice (27,28). A case of previous study has also reported that OSR exerts antioxidant and anti-inflammatory effects in Alzheimer's disease by targeting the TLR4/NF- κ B signaling pathway and TLR4-specific inhibitor TAK-242 effectively enhances the effects of OSR (23).

Another study reported that TAK-242 serves a neuroprotective and anti-ferroptotic role by inhibiting TLR4/p38MAPK signaling in hypoxic-ischemic brain injury (29). In the present study, I/R or OGD/R treatment induced production of TLR4, MyD88 and p-p38, but OSR significantly decreased expression levels of these proteins, which suggested that OSR exerted an inhibitory effect on the TLR4/p38MAPK signaling pathway in cerebral I/R injury.

Ferroptosis is a modulated form of cell death characterized by lethal iron-dependent accumulation of lipid peroxides and is involved in several types of brain disease, including cerebral I/R (30). Guan *et al* (31) reported that carvonol exerts a neuroprotective effect on I/R-induced hippocampal neuronal injury by alleviating ferroptosis. Guo *et al* (32) reported that carthamin yellow protects rats against cerebral I/R injury by inhibiting inflammation and ferroptosis in a MCAO model. In the present study, I/R and OGD/R significantly increased ROS, ATP, Fe²⁺, ACSL4 and TFR1 levels and significantly decreased FTH1 and GPX4 levels, thereby inducing neuronal ferroptosis. OSR inhibited expression of ferroptosis-associated proteins, attenuated oxidative stress, decreased the pro-inflammatory response and ameliorated activation of hippocampal neuronal ferroptosis. However, TLR4 overexpression and treatment with the p38MAPK activator anisomycin both significantly exacerbated OGD-induced oxidative stress and ferroptosis, which suggested that the TLR/p38MAPK signaling pathway mediated the ferroptotic process following I/R and OGD/R exposure and that this signaling pathway was regulated by OSR. In the study, the effects of TLR4/p38MAPK overexpression on OGD-induced ferroptosis in OSR-treated cells were evaluated but the effects of this pathway on OGD/R-induced viability, oxidative stress and inflammatory response in OSR-treated cells was not assessed. Moreover, there was a lack of validation at the mitochondrial level and there was no detection of lipid peroxidation products. Further work is required to evaluate the effect of TLR4/p38MAPK on other functional roles in OGD/R-induced neuronal cells with or without OSR, verify the results of the present study at the mitochondrial level and detect lipid peroxidation products.

In conclusion, the results of the present study indicated that OSR attenuated brain injury and neuronal apoptosis, oxidative stress and inflammatory response in cerebral I/R injury by inhibiting ferroptosis. Moreover, OSR decreased OGD/R-induced neuronal ferroptosis by inactivation of the TLR4/p38MAPK signaling pathway.

Acknowledgements

Not applicable.

Funding

This work was supported by Zhejiang TCM Science and Technology Project (grant no. 2023004198).

Availability of data and materials

The datasets used and/or analyzed during the current study are available from the corresponding author on reasonable request.

Authors' contributions

JZ and MM designed the study and drafted and revised the manuscript. LL and GF analyzed the data and reviewed the literature. JZ and MM confirmed the authenticity of all the raw data. All authors performed the experiments. All authors have read and approved the final manuscript.

Ethics approval and consent to participate

All procedures using animals were approved by the Animal Care and Use Committee of Hangzhou Red Cross Hospital (approval no. 20220414) and performed in accordance with Chinese legislation regarding experiment animals.

Patient consent for publication

Not applicable.

Competing interests

The authors declare that they have no competing interests.

References

- Liu W, Wong A, Law AC and Mok VC: Cerebrovascular disease, amyloid plaques, and dementia. *Stroke* 46: 1402-1407, 2015.
- Lanzino G and Brown RD Jr: Introduction: Management of ischemic cerebrovascular disease. *Neurosurg Focus* 36: 1-2, 2014.
- Wang L, Jia J, Hong Z, Zhang L and Zhang J: Effects of chemerin and homocysteine levels and their associations with occurrence and development of ischemic cerebrovascular disease. *Lipids Health Dis* 20: 108, 2021.
- Lu J and Wang DM: Update in endovascular therapy of ischemic cerebrovascular disease. *Zhonghua Wai Ke Za Zhi* 59: 192-195, 2021 (In Chinese).
- Lim S, Kim TJ, Kim YJ, Kim C, Ko SB and Kim BS: Senolytic Therapy for cerebral ischemia-reperfusion injury. *Int J Mol Sci* 22: 11967, 2021.
- Yang Z, Weian C, Susu H and Hanmin W: Protective effects of mangiferin on cerebral ischemia-reperfusion injury and its mechanisms. *Eur J Pharmacol* 771: 145-151, 2016.
- Banz Y and Rieben R: Role of complement and perspectives for intervention in ischemia-reperfusion damage. *Ann Med* 44: 205-217, 2012.
- Al-Mufti F, Amuluru K, Roth W, Nuoman R, El-Ghanem M and Meyers PM: Cerebral ischemic reperfusion injury following recanalization of large vessel occlusions. *Neurosurgery* 82: 781-789, 2018.
- Yao XQ, Zhang YH, Long W and Liu PX: Oxysophoridine suppresses the growth of hepatocellular carcinoma in mice: In vivo and cDNA microarray studies. *Chin J Integr Med* 18: 209-213, 2012.
- Wang R, Deng X, Gao Q, Wu X, Han L, Gao X, Zhao S, Chen W, Zhou R, Li Z and Bai C: *Sophora alopecuroides* L.: An ethnopharmacological, phytochemical, and pharmacological review. *J Ethnopharmacol* 248: 112172, 2020.
- Meng C, Liu C, Liu Y and Wu F: Oxysophoridine attenuates the injury caused by acute myocardial infarction in rats through anti-oxidative, anti-inflammatory and anti-apoptotic pathways. *Mol Med Rep* 11: 527-532, 2015.
- Cao Z, Chen L, Liu Y and Peng T: Oxysophoridine rescues spinal cord injury via anti-inflammatory, anti-oxidative stress and anti-apoptosis effects. *Mol Med Rep* 17: 2523-2528, 2018.
- Wang H, Li Y, Jiang N, Chen X, Zhang Y, Zhang K, Wang T, Hao Y, Ma L, Zhao C, *et al*: Protective effect of oxysophoridine on cerebral ischemia/reperfusion injury in mice. *Neural Regen Res* 8: 1349-1359, 2013.
- Zhai Z and Feng J: Left-right asymmetry influenced the infarct volume and neurological dysfunction following focal middle cerebral artery occlusion in rats. *Brain Behav* 8: e01166, 2018.

15. Livak KJ and Schmittgen TD: Analysis of relative gene expression data using real-time quantitative PCR and the 2(-Delta Delta C(T)) method. *Methods* 25: 402-408, 2001.
16. Mehanna R and Jankovic J: Movement disorders in cerebrovascular disease. *Lancet Neurol* 12: 597-608, 2013.
17. Sveinsson OA, Kjartansson O and Valdimarsson EM: Cerebral ischemia/infarction-epidemiology, causes and symptoms. *Laeknabladid* 100: 271-279, 2014 (In Icelandic).
18. Suzuki H, Kanamaru H, Kawakita F, Asada R, Fujimoto M and Shiba M: Cerebrovascular pathophysiology of delayed cerebral ischemia after aneurysmal subarachnoid hemorrhage. *Histol Histopathol* 36: 143-158, 2021.
19. Qin Y, Zhang Q and Liu Y: Analysis of knowledge bases and research focuses of cerebral ischemia-reperfusion from the perspective of mapping knowledge domain. *Brain Res Bull* 156: 15-24, 2020.
20. Kawadkar M, Mandloi AS, Saxena V, Tamadaddi C, Sahi C and Dhote VV: Noscapine alleviates cerebral damage in ischemia-reperfusion injury in rats. *Naunyn Schmiedebergs Arch Pharmacol* 394: 669-683, 2021.
21. Guan X, Li Z, Zhu S, Cheng M, Ju Y, Ren L, Yang G and Min D: Galangin attenuated cerebral ischemia-reperfusion injury by inhibition of ferroptosis through activating the SLC7A11/GPX4 axis in gerbils. *Life Sci* 264: 118660, 2021.
22. Wang G, Wang T, Zhang Y, Li F, Yu B and Kou J: Schizandrin protects against OGD/R-induced neuronal injury by suppressing autophagy: Involvement of the AMPK/mTOR pathway. *Molecules* 24: 3624, 2019.
23. Chen R, Wang Z, Zhi Z, Tian J, Zhao Y and Sun J: Targeting the TLR4/NF- κ B pathway in β -amyloid-stimulated microglial cells: A possible mechanism that oxysophoridine exerts anti-oxidative and anti-inflammatory effects in an in vitro model of Alzheimer's disease. *Brain Res Bull* 175: 150-157, 2021.
24. Rui C, Yuxiang L, Ning J, Ningtian M, Qingluan Z, Yinju H, Ru Z, Lin M, Tao S and Jianqiang Y: Anti-apoptotic and neuroprotective effects of oxysophoridine on cerebral ischemia both in vivo and in vitro. *Planta Med* 79: 916-923, 2013.
25. Wang TF, Lei Z, Li YX, Wang YS, Wang J, Wang SJ, Hao YJ, Zhou R, Jin SJ, Du J, *et al*: Oxysophoridine protects against focal cerebral ischemic injury by inhibiting oxidative stress and apoptosis in mice. *Neurochem Res* 38: 2408-2417, 2013.
26. Iadecola C and Anrather J: The immunology of stroke: From mechanisms to translation. *Nat Med* 17: 796-808, 2011.
27. Liu J, Chen Q, Jian Z, Xiong X, Shao L, Jin T, Zhu X and Wang L: Daphnetin protects against cerebral ischemia/reperfusion injury in mice via inhibition of TLR4/NF- κ B signaling pathway. *Biomed Res Int* 2016: 2816056, 2016.
28. Caso JR, Pradillo JM, Hurtado O, Lorenzo P, Moro MA and Lizasoain I: Toll-like receptor 4 is involved in brain damage and inflammation after experimental stroke. *Circulation* 115: 1599-1608, 2007.
29. Zhu K, Zhu X, Sun S, Yang W, Liu S, Tang Z, Zhang R, Li J, Shen T and Hei M: Inhibition of TLR4 prevents hippocampal hypoxic-ischemic injury by regulating ferroptosis in neonatal rats. *Exp Neurol* 345: 113828, 2021.
30. Stockwell BR, Friedmann Angeli JP, Bayir H, Bush AI, Conrad M, Dixon SJ, Fulda S, Gascón S, Hatzios SK, Kagan VE, *et al*: Ferroptosis: A regulated cell death nexus linking metabolism, redox biology, and disease. *Cell* 171: 273-285, 2017.
31. Guan X, Li X, Yang X, Yan J, Shi P, Ba L, Cao Y and Wang P: The neuroprotective effects of carvacrol on ischemia/reperfusion-induced hippocampal neuronal impairment by ferroptosis mitigation. *Life Sci* 235: 116795, 2019.
32. Guo H, Zhu L, Tang P, Chen D, Li Y, Li J and Bao C: Carthamin yellow improves cerebral ischemia-reperfusion injury by attenuating inflammation and ferroptosis in rats. *Int J Mol Med* 47: 52, 2021.



This work is licensed under a Creative Commons Attribution-NonCommercial-NoDerivatives 4.0 International (CC BY-NC-ND 4.0) License.